Effects of optical beam angle on quantitative optical coherence tomography (OCT) in normal and surface degenerated bovine articular cartilage

Short title: Effects of beam angle on quantitative OCT of articular cartilage

Yan-Ping Huang[1,2,5], Simo Saarakkala[2,4], Juha Toyras[2,3], Li-Ke Wang[1], Jukka S. Jurvelin[2], and Yong-Ping Zheng[1]

E-mail: hti.huang@polyu.edu.hk

[1] Department of Health Technology and Informatics, Hong Kong Polytechnic University, Hong Kong, China
[2] Department of Physics and Mathematics, University of Eastern Finland, Kuopio, Finland
[3] Department of Clinical Neurophysiology, Kuopio University Hospital, Kuopio, Finland
[4] Department of Diagnostic Radiology, University of Oulu, Oulu, Finland

Revision #1 submitted to *Physics in Medicine and Biology* as *paper*, Nov 2010

---

[5] Author to whom any correspondence should be addressed

Abstract

Quantitative measurement of articular cartilage using optical coherence tomography (OCT) is a potential approach for diagnosing the early degeneration of cartilage and assessing the quality of its repair. However, a non-perpendicular angle of the incident optical beam with respect to the tissue surface may cause uncertainty to the quantitative analysis and, therefore, significantly affect the reliability of measurement. This non-perpendicularity was systematically investigated in the current study using the bovine articular cartilage with and without mechanical degradation. Ten fresh osteochondral disks were quantitatively measured before and after artificially induced surface degradation by mechanical grinding. The following quantitative OCT parameters were determined with a precise control of the surface inclination up to an angle of 10° using a step of 2°: optical reflection coefficient (*ORC*), variation of surface reflection along the surface profile (*VSR*), optical roughness index (*ORI*), and optical backscattering (*OBS*). It was found that non-perpendicularity caused systematic changes to all of the parameters. *ORC* was the most sensitive and *OBS* the most insensitive to the inclination angle, respectively. At the optimal perpendicular angle, all parameters could detect significant changes after surface degradation ($p < 0.01$), except *OBS* ($p > 0.05$). Nonsignificant change of *OBS* after surface degradation was expected since *OBS* reflected properties of the internal cartilage tissue and was not affected by the superficial mechanical degradation. As a conclusion, quantitative OCT parameters are diagnostically potential for characterizing the cartilage degeneration. However, efforts through a better controlled operation or corrections based on computational compensation mechanism should be made to minimize the effects of non-perpendicularity of the incident optical beam when clinical use of quantitative OCT is considered for assessing the articular cartilage.

1. Introduction

Optical coherence tomography (OCT) is a fast developing technique having widespread applications in imaging small scale biological soft tissues (Fujimoto *et al.*, 2000). This technique has also been successfully applied to the imaging of articular cartilage *in vivo* due to its easy access through an arthroscopic operation (Herrmann *et al.*, 1999; Pan *et al.*, 2003). The potential of this modality for the diagnosis of early degeneration of cartilage involved in osteoarthritis (OA) (Chu *et al.*, 2007; Chu *et al.*, 2010) and for the assessment of cartilage repair (Han *et al.*, 2003) has also been earlier investigated. The advantages of this technique, compared to other imaging modalities, mainly come from its high resolution from a few to several tens of microns, which is potential for the operation of 'optical biopsy' without tissue dissection. Some of previous studies have focused on comparing between OCT and histological images (Chu *et al.*, 2004; Han *et al.*, 2003; Li *et al.*, 2005; Patel *et al.*, 2005; Xie *et al.*, 2006a) and exploring some advanced modes such as the polarization sensitive OCT for the detection of collagen disorganization in articular cartilage (Chu *et al.*, 2007; Drexler *et al.*, 2001; Liu *et al.*, 2006; Patel *et al.*, 2005; Xie *et al.*, 2006a; Xie *et al.*, 2008). Recent studies have focused on quantitative characterization of articular cartilage and its OA-like degeneration using morphologic and optical parameters obtained using OCT. Among them, the cartilage thickness has become the first quantitative and apparently meaningful parameter to be extracted from the OCT imaging of cartilage (Han *et al.*, 2003; Herrmann *et al.*, 1999; Rogowska *et al.*, 2003). Algorithms for automatic delineation of cartilage surface and cartilage-bone interface in OCT images have been proposed to calculate the cartilage thickness thereof (Rogowska and Brezinski, 2002; Rogowska *et al.*, 2003). Other morphologic parameters such as the hypertrophic regeneration index and the fibrillation index (Chu *et al.*, 2004; Han *et al.*, 2003) and optical parameters, such as the refractive index of articular cartilage (Wang *et al.*, 2010b), were also proposed in quantitative studies. In this respect, we have recently proposed two quantitative parameters: the surface optical reflection coefficient

(*ORC*) and surface optical roughness index (*ORI*), for the quantification of degeneration in articular cartilage using OCT (Saarakkala *et al.*, 2009).

The basic working principle of OCT is similar to that of ultrasound in the pulse-echo mode, which detects the reflection/backscattering from different depths of the tested material for the purpose of imaging. For quantitative analysis of the reflected/backscattered signal, especially from an interface where reflection may dominate, effects of the incident beam angle are always of concern. This is also the case for quantitative OCT. Consequently, it is of paramount importance to study those effects to get an understanding of the sensitivity of OCT measurements. The influence of beam incidence angle has been reported for the polarization sensitive OCT (Fanjul-Velez and Arce-Diego, 2010; Ugryumova *et al.*, 2009; Xie *et al.*, 2006b). The polarization sensitive OCT is a potential technique to detect the collagen fiber orientation nondestructively and *in vivo* for articular cartilage. Xie et al. (2006) showed that the pattern of phase retardation with cartilage depth varies significantly with respect to the change of the optical beam angle to the cartilage surface (Xie *et al.*, 2006b). Other than the polarization sensitivity, experimental data addressing the influence of the optical beam angle on other quantitative OCT parameters are still limited. In ultrasound, such studies of angle dependence on liver (Waag *et al.*, 1982), breast (Davros *et al.*, 1986) and myocardial tissues (Hiro *et al.*, 1999; Picano *et al.*, 1985) have been reported. High frequency ultrasound has also been proposed as a potential method for assessing the physical status of articular cartilage (Adler *et al.*, 1992; Chiang *et al.*, 1994). An ultrasound roughness index (*URI*) has been adopted for quantitatively studying the cartilage degradation (Saarakkala *et al.*, 2004). Specifically, the effects of acoustic beam incidence angle and surface roughness on the quantitative ultrasound parameters of articular cartilage have been reported in a recent study (Kaleva *et al.*, 2009), and the importance of beam perpendicularity in ultrasound measurement has been demonstrated thereof. However, considering the difference of physics between ultrasound and light and the difference of changes of acoustic and optical properties at the cartilage surface, the results related to ultrasound are not directly applicable to the OCT measurement on articular cartilage.

The aims of the current study are to investigate the effects of optical beam angle on the quantitative optical parameters obtained using OCT in normal and degenerated articular cartilage. Both intact and surface degraded articular cartilages were tested with a broad range of non-perpendicular incidence angles. The results were then analyzed to depict how the beam non-perpendicularity would affect the quantitative OCT characterization of both the surface and the internal cartilage tissues.

2. Materials and methods

2.1. Sample preparation and processing

Fresh bovine knees of young mature bulls (age range = 1-3 years) were obtained from a local abattoir (Atria Oyj, Kuopio, Finland) and opened within a few hours post mortem. If there were any visual signs of OA on the cartilage surfaces, or disruption of the joint capsule, this knee would be excluded from the study. From each patella, two osteochondral disks (diameter = 6 mm) with a total thickness of approximately 4 mm were extracted from the visually intact lateral upper quadrant. A total of 20 (n = 10 × 2) disks were prepared. During the sample preparation, the patellae were hydrated with phosphate buffered physiological saline solution (PBS). After preparation, the samples were immediately immersed in PBS with inhibitors of metalloproteinases containing 5 mM ethylenediaminetetraacetic acid (EDTA) disodium salt (VWR International, Fontenay, France) and 5 mM benzamidine hydrochloride (Sigma-Aldrich Inc., St. Louis, MO, USA) and stored there until measurement. All the disks were measured using OCT within the same day of preparation. For the two disks of each patella, one served as control (C) and the other as an experiment sample (E). For C disk, three repeated measurements were conducted to test the reproducibility of the measured parameters. E disk was first measured using different depths of bathing PBS to investigate the effects of PBS immersion. Subsequently, it was tested with various angles of surface inclination to study the effects of non-perpendicular optical beam incidence. After that, E disks were manually ground with emery paper (P120, PEPA standard; average particle size: 125 μm) along two perpendicular directions, to simulate the early degeneration, *i.e.*, fibrillation of the cartilage surface. After grinding, measurements with different angles of inclination were performed again. Finally after all the measurements, the samples (both C and E) were cut in halves, one sent for scanning electron microscopy (SEM) and the other for histology (Safranin O staining).

2.2. OCT system and testing setup

A time-domain OCT system (developed by the Lab of Optical Imaging and Sensing, Graduate School at Shenzhen, Tsinghua University, China) was employed for the imaging in this study (Saarakkala *et al.*, 2009). The system used a 1310 nm superluminescent diode with a bandwidth of 50 nm, corresponding to an axial resolution of approximately 15 μm in free space propagation. The OCT probe, which included optical fibers, compound lenses and a scanning mirror, could be translated vertically to adjust the distance between the probe and the tested material. A red light was also coupled with the infrared light for guiding the testing point. OCT signals were digitized at a sampling rate of 500 kS/s by a data acquisition card (PCMCIA 6062E, National Instruments, Austin, TX, USA) installed in a notebook. They were collected by a custom-designed Labview program (v8.0, National Instruments, Austin, TX, USA) and saved for offline analysis with custom written Matlab (v.R2008a, Mathworks, Inc., Natick, MA, USA) scripts using a graphic user interface (GUI). In this study, one cross-sectional scan was composed of 100 axial lines (A-lines) covering a lateral width of 1.0 mm. At each testing site, totally three repeated tests were collected and the mean result was used for this site. Each A-line included 4255 data points in the axial direction. Through calibration, one interval between two consequent data points represented an equivalent distance of 1.228 μm and 0.933 μm in air and PBS, respectively.

Figure 1 shows the basic measurement setup for the surface inclination test. A glass container with a diameter of 4 cm was installed on top of three mechanical devices for adjusting the position at the horizontal plane (Stage A1 & A2), the inclination of the sample surface (Stage B) and the scan direction (Stage C). On the bottom were two manual linear stages (Stage A1 & A2, 4400 Series, Parker Hannifin Corp., Cleveland, OH, USA) adjustable in two perpendicular directions with a maximum range of 50 mm in the horizontal plane. In the middle was a goniometer (Stage B, Model 55-840, Edmund Optics Inc, Barrington, NJ, USA) with a maximum range of 20° for adjusting the surface inclination of the cartilage. On the top was a rotary stage (Stage C, Model 7SRM173, 7 Star Optical Instruments Co. Ltd., Beijing, China) with a 360° free rotation for adjusting the scan direction for OCT imaging. During the measurement, the testing point was adjusted to be at the intersection of the two rotation centers of Stage B and Stage C, to assure that the same point was tested at different surface inclinations and scan directions.

2.3. Experiments

In trial tests, it was found that the OCT signal from cartilage surface was much smaller when the test was conducted in bathing PBS compared to that performed directly on cartilage without PBS. As a preliminary test, we therefore studied the effect of bathing PBS by observing whether the decrease of amplitude was caused by the attenuation of PBS or by different interfaces (cartilage-PBS versus cartilage-air). The osteochondral disk (E) was installed at the center of the container with fast curing adhesive glue (Pika-Liima, Kiilto Oy, Tampere, Finland). PBS on the cartilage surface was blown off by a manual dust blower at first and the signals were then measured in air (PBS depth = 0). Subsequently, the samples were tested with a PBS depth of approximately 2, 4, 6 and 8 mm by injecting a fixed volume of PBS (about 2.5 ml) step by step into the container. After that, the PBS was drained with a syringe from the side of the container, but naturally leaving a very thin layer of PBS on the surface of the cartilage, and signals were collected again.

The real thickness l of the PBS layer over the cartilage could be calculated based on OCT images by:

$$l = \frac{\Delta l}{2(n_{PBS} - n_{air})}, \qquad (1)$$

where Δl is the free space distance of the shift of the cartilage surface compared to its initial position without PBS, and n_{PBS} and n_{air} are the refractive indices of PBS and air, respectively. Values of n_{PBS} and n_{air} measured in this study are given in the next subsection. At each depth of PBS, the signals were collected at the center of the osteochondral disk with 4 scan directions by adjusting Stage C at angles of 0°, 45°, 90° and 135° (figure 1). No adjustment of Stage B was performed during the measurement to assure that all the changes originated from the change of bathing PBS but not that of the surface inclination. All the disks were set at the same distance (≈ 7 cm) from the OCT probe which was judged by the same position of the cartilage surface observed in the OCT image when no PBS was present.

After studying the effects of PBS immersion, we decided not to bathe the cartilage layer in PBS (figure 1) during the subsequent measurements in order to increase the signal to noise ratio (*SNR*) of the collected OCT signals. The cartilage (E) disk was fixed by the same type of glue as mentioned above at the center of the container. To keep the cartilage tissue moistened during the measurements, some PBS was filled at the bottom of the container at a level up to the cartilage-bone interface and the container was sealed on top by a very thin cling film (Serla, Metsa Tissue Co., Espoo, Finland). Before testing, PBS on the cartilage surface was blown off by the dust blower to get optimal signals. For the installation of each disk, the testing point was placed on the centers of rotation for both Stage B and Stage C. Four series of scan with different directions of 0°, 45°, 90° and 135° (figure 1) were performed for each E disk. At each direction, the cartilage surface was firstly oriented by Stage B to be perpendicular to the optical beam by observing a maximum OCT signal from the cartilage surface. This angle was assumed to be 0° for the cartilage surface. Then signals were also collected with the inclination angles of 2°, 4°, 6°, 8° and

10° by precisely rotating Stage B. After that, the same measurements were performed at the next scan direction by a rotation of 45° for Stage C. This type of data collection was repeated for the four scan directions. At each scan direction, the adjustment of perpendicularity was conducted before the data collection. The total time for each E disk measurement was about 15 min. After all the tests, the E disk was mechanically ground and immersed in PBS for at least 15 min. Then the same OCT measurements were repeated for different scan directions and different angles of inclination. The averaged results of the four scan directions were used for the comparison of optical parameters among different inclination angles and before and after mechanical degradation of cartilage surface. As a reference, a piece of very smooth microscopy slide was also scanned using similar protocols as the cartilage. All the measurements were conducted at room temperature 21 ± 1ºC.

In order to investigate the reproducibility of measured optical parameters, three repeated scans were also performed on each C sample at an optimal angle of inclination. Among these three tests, the cartilage was firstly changed to a big inclination angle of at least 10° and then re-oriented to the optimal inclination angle by observing a maximum signal amplitude. After the tests, all C and E samples were cut into two halves for SEM and histology studies, respectively.

2.4. Extraction of quantitative parameters

In this study, four parameters were calculated to quantitatively characterize the OCT signals from both the cartilage surface and the internal tissue before and after mechanical grinding: surface optical reflection coefficient (*ORC*), variation of surface reflection along the surface profile (*VSR*), surface optical roughness index (*ORI*), and optical backscattering (*OBS*) of the internal tissue. Recorded optical signals were analyzed offline in a self-designed Matlab GUI. Two windows were manually drawn on the cartilage image in order to guide the subsequent automatic detection of the surface profile (figure 2). The width of both windows was set in default to 1 mm, *i.e.* full width of the scan. The first window (noise window, in air) of about 300 points in depth was used to define the noise level and the second window (cartilage window) of about 1500 points in depth included the cartilage surface and a part of the cartilage layer. For each testing site, the signal envelopes obtained using a Hilbert transform were calculated for the three repeated measurements and averaged. Subsequently, one single image with a total of 100 envelope signal lines was obtained for detecting the surface profile in a line-by-line manner. A mean noise value was obtained by averaging the signal values in the noise window. For detection of the surface profile at each signal line, a maximum value of the signal in the cartilage window was determined. In this study, the surface start point was detected by using a predefined threshold: noise mean + 30% of the maximum value in the cartilage window in a search direction from air to cartilage. After detecting the surface start point, the maximum value in the following 200 points (about 0.2 mm) was determined and denoted by A_i, where i stands for the i^{th} line of the scanned image. The corrected surface reflection coefficient (*ORC*) for this line was obtained by normalizing it to a reference value at the same depth:

$$ORC_i = \frac{A_i}{A_{i,c}}, \tag{2}$$

where $A_{i,c}$ is a reference signal amplitude from a perfect reflector at the same distance. This reference signal was measured in an indirect way: it was calculated based on the amplitude collected from a glass slide and the reflection coefficient estimated from the refractive indices of slide and air. At least 20 reference signals at different distances covering the measurement range were collected and the reference amplitude at any distance was obtained simply by a linear interpolation of the amplitudes between two measured points. The *ORC* was then calculated as the spatial average of ORC_i along the 100 lines and the variation of surface reflection (*VSR*, %) was calculated as the coefficient of variance for ORC_i along the surface profile, respectively:

$$ORC = \frac{1}{N}\sum_i ORC_i\ , \tag{3}$$

$$VSR = \frac{SD \text{ of } ORC_i}{ORC} \times 100\,\% \quad , \tag{4}$$

where $N = 100$ is the total number of signal lines. For each disk at different angles of surface inclination, the ORC was logarithmically converted into decibels (dB) for final comparisons.

In order to obtain the optical roughness index (*ORI*) of the cartilage surface, the surface profile was first filtered by a moving average of 20 points (0.2 mm) to obtain a smoothed surface, indicated by $\overline{d}_i$ at line i (figure 2). A filtered surface profile reflecting the true surface roughness of articular cartilage was obtained by the following operation:

$$D_i = d_i - \overline{d}_i \,, \tag{5}$$

where D_i is surface position after filtering, and d_i is the originally detected position at line i. The ORI was calculated based on the final surface profile using the following equation (Saarakkala *et al.*, 2009):

$$ORI = \sqrt{\frac{1}{N}\sum_i D_i^2} \,. \tag{6}$$

The optical backscattering (*OBS*) was defined as the averaged backscattered signal level in a 500-point region of interest (ROI) under the cartilage surface. This parameter was calculated based on the original OCT signal rather than its envelope. The start of ROI was chosen as the point which was 100 points (about 0.1 mm) after the originally detected surface point. The *OBS* at line i is calculated as:

$$OBS_i = \frac{1}{(1 - ORC_i^2)^2} \cdot \frac{1}{M} \sum_j \overline{b}_{i,j}^2 \,, \tag{7}$$

where $b_{i,j}$ is the original OCT signal value at point *j* of line *i* and *M* = 500 is the total number of points for averaging at line *i*. $\overline{b}_{i,j}^2$ was obtained by averaging the three repeated tests at each point. The factor $(1 - ORC_i^2)^2$ was used to approximately compensate the energy loss of double reflections (forward and backward) at the cartilage surface. The OBS_i was then averaged for the 100 lines to obtain *OBS* and converted into a unit of dBV for final comparisons.

In this study, refractive indices of the light in air, PBS and slide were determined through a calibration test (Wang *et al.*, 2010b). Values of 1, 1.316 and 1.544 were used to represent the refractive index of air, PBS and glass slide, respectively. These values were used to calculate the depth of PBS and also an estimation of the surface inclination angles based on OCT images. For reference, the true experimental inclination angle was also estimated from the extracted surface profile. A straight line was fitted to the original surface profile and the angle of this line was computed as a real inclination angle with respect to the incident optical beam.

2.5. Scanning electron microscopy and histology

Surfaces of control and mechanically degraded cartilage were imaged at a magnification of ×200 using a scanning electron microscope (SEM) (Philips XL30 ESEM, Fei Co., Eindhoven, Netherlands). Before SEM, the samples were fixed in 2% glutaraldehyde buffered with 0.1 mol/l cacodylate (pH 7.4), dehydrated in an ascending series of ethanol solutions, dried using the critical point technique and coated with a sputtered gold layer (Jurvelin *et al.*, 1983).

To evaluate the histological status and proteoglycan content of the samples, Safranin O stained slices (thickness = 3 μm) were digitally imaged with a pixel size of 2.58 μm using an optical microscope (Axio Imager M2, Zeiss, Germany). Custom-written MATLAB scripts were then used to trace the surface profile from the digitized histological images based on detection of an abrupt color change at the cartilage surface. Root-mean-square roughness values were then calculated from the surface profile in a way similar to that of the *ORI* to gain reference values of the surface roughness for the OCT measurement.

2.6. Statistical analysis

A standardized coefficient of variation (*SCV*) was used to assess the reproducibility of measured OCT parameters in normal cartilage samples (Fournier *et al.*, 2001; Wang *et al.*, 2010a):

$$SCV = \frac{CV \cdot \bar{x}_{1st}}{4 \cdot SD_{1st}}, \tag{8}$$

where $\bar{x}_{1st}$ and SD_{1st} are, respectively, the mean and the standard deviation of the measured parameter where only the first measurement is taken into account. *CV* is the global coefficient of variance, which is defined as:

$$CV = \sqrt{\frac{\sum_i SD_i^2}{m}} \Bigg/ \frac{\sum_i \bar{x}_i}{m}, \tag{9}$$

where $\bar{x}_i$ and SD_i are, respectively, the mean and the standard deviation for the *n* repeated measurements in sample *i*, and *m* is the total number of samples. In this study, $n = 3$ indicated three repeated tests in each C disk and $m = 10$ was the total number of disks.

All the optical parameters at angles other than 0° were compared with those at the perpendicular angle (0°) using paired-sample *t*-test to observe the effects of non-perpendicular beam incidence. The parameters were also compared using the paired-sample *t*-test before and after the mechanical grinding of the samples at the surface inclination angle of 0°. All the statistical analyses were performed with SPSS (15.0 for Windows, SPSS Inc., Chicago, IL, USA). A level of $p < 0.05$ was used to indicate a significant difference.

3. Results

*SCV*s for *ORC*, *VSR*, *ORI* and *OBS* were 8.1%, 7.4%, 13.5% and 2.1%, respectively. Effect of the PBS immersion on the OCT signal was estimated only for *ORC*. The averaged PBS depths at the six steps of measurements were 0, 0.16 ± 0.07 mm, 1.27 ± 0.30 mm, 3.34 ± 0.31 mm, 5.41 ± 0.30 mm and 7.55 ± 0.32 mm from (1). When normalized to its value without PBS, *ORC* at the six PBS depths was 0, -16.8 ± 2.1 dB, -18.4 ± 2.1 dB, -20.6 ± 2.3 dB, -22.7 ± 2.4 dB and -24.9 ± 2.3 dB, respectively. Therefore, it was shown that the main cause of a poor signal quality for cartilage measured in PBS was the change of the interface from air/cartilage to PBS/cartilage.

Figure 2 shows typical images and surface profiles obtained from intact cartilage at 0º and 10º inclinations and surface degraded cartilage at 0º inclination. Decreased signal amplitude at a larger inclination angle and a roughened surface after grinding were obviously observed. Quantitative analyses confirmed these findings. Results for the quantitative parameters are shown in figures 3-6. The comparisons between parameters at non-zero angles with those at 0º are tabulated in table 1. *ORC* showed a distinct negative correlation with the inclination angle (figure 3). The intact cartilage, similar to the slide, showed a larger slope than the degraded cartilage (-2.02 dB/degree vs. –0.94 dB/degree). There was a slight decrease of *VSR* with the increase of the inclination angle (figure 4). An evident increase of *ORI* with the increase of the inclination angle was observed (figure 5). This angle dependence was slightly larger in the intact group (0.96 μm/degree) than that in the degraded group (0.70 μm/degree). *OBS* showed a slight decrease with the increase of the inclination angle (figure 6), for which the trend was similar to that of *ORC*. The trend in the intact cartilage was similar to that in the degraded cartilage (-0.08 dBV/degree vs. –0.06 dBV/degree), but was much smaller than that of *ORC*. For reference, the true surface inclination angle estimated from the OCT images was 0.8 ± 0.9º, 2.8 ± 0.8º, 4.8 ± 0.9º, 6.7 ± 1.2º, 8.6 ± 1.4º and 10.4 ± 1.8º in the intact cartilage and 1.6 ± 2.7º, 4.0 ± 2.7º, 6.1 ± 2.4º, 8.3 ± 2.2º, 10.5 ± 2.1º and 12.3 ± 2.2º in the degraded cartilage, respectively. This demonstrated that the adjustment of the surface inclination using the goniometer based on the current setup was quite successful.

OCT parameters at the optimized perpendicular angle (0º) are listed in table 2. With an optimal data collection, all the parameters could differentiate the degraded cartilage from the intact cartilage except *OBS*, which was not affected by the mechanical grinding process. However, at non-perpendicular angles, *ORC* was significantly affected and might not allow separation of intact and degenerated tissue at a large inclination angle. However, the separation of intact and degenerated tissue was possible at all investigated angles for *VSR* and *ORI*.

Typical SEM and histological images are shown in figure 7 and figure 8, respectively. From the SEM images, it can be clearly observed that the cartilage surface was damaged after the mechanical grinding. The Safranin O stained sections revealed that the degradation was limited only to the cartilage surface and did not affect the proteoglycan content of the internal tissue. Roughness values obtained from the histological images are also shown in table 2, and they were quite consistent with *ORI* values. The roughness of the cartilage surface from the histological images also showed a significant increase after the mechanical grinding ($p < 0.001$).

4. Discussion

Quantitative characterization of biological tissues using OCT has a great potential for the detection of early degeneration of articular cartilage (Chu *et al.*, 2004; Han *et al.*, 2003; Saarakkala *et al.*, 2009; Wang *et al.*, 2010b). In this study, the effects of the non-perpendicular optical beam on the proposed quantitative OCT parameters were investigated in normal and surface degraded bovine articular cartilage. Results showed that while some of the studied parameters are more robust to the inclination angle than others, special control of the inclination angle or inclination angle-based compensation mechanism is necessary if those sensitive parameters, *e.g. ORC*, will be considered. The results of the current investigation can serve as a reference for future studies in an effort to enable the clinical use of quantitative OCT.

4.1. Reproducibility of measurements

Results of *SCV* showed that the reproducibility was the highest for *OBS* and the lowest for *ORI*. This was understandable considering that *OBS* was obtained by averaging quite a lot of data points while *ORI* was calculated based on a single surface profile at each testing site. It should be noted that *ORI* of the glass slide was about 2.0 μm. Considering its true roughness being much smaller than this value, it was hypothesized that *ORI* = 2.0 μm was the resolution for roughness measurement with the current OCT system. This was also the case in the intact cartilage as roughness values of 0.8 μm had been reported for the healthy bovine cartilage in the literature (Forster and Fisher, 1999). Furthermore, intact cartilage surfaces might be quite smooth so the inter-sample variation was quite small, which correspondingly increased the *SCV* according to (8). Therefore, considering big differences of surface reflection and roughness between intact and degraded articular cartilage and a better control of the measurement process such as the optical beam incidence, the reproducibility of the OCT measurements was generally acceptable for detecting the early degeneration of cartilage.

4.2. Effects of PBS immersion

It was found that the existence of a PBS layer induced a significant drop in the signal amplitude of the surface reflection (about -16.8 dB for *ORC*). This decrease was significantly larger than that induced by the attenuation (about -1.1 dB/mm) of PBS of several millimeters in depth. The most probable reason for the large effect of PBS was the change of refractive index at the cartilage surface. When the interface was cartilage/PBS, the reflection coefficient, according to the Fresnel Equation with a normal incidence, was about $\alpha_1 = \left|(n_{PBS} - n_{cartl}) \;/\; (n_{PBS} + n_{cartl})\right| \approx$ 0.016, based on a mean value of $n_{cartl} = 1.358$ for the normal cartilage (Wang *et al.*, 2010b). However, when the interface was cartilage/air, the reflection coefficient was $\alpha_2 = \left|(n_{air} - n_{cartl}) \;/\; (n_{air} + n_{cartl})\right| \approx$0.136. The theoretical change of reflection coefficient was $\Delta = 20\log(\alpha_2/\alpha_1) = 18.6\,\mathrm{dB}$, which was quite close to the value measured in the current study. As no gain adjustment was available in the current OCT system and a low *SNR* was observed when the cartilage was measured in PBS, testing without immersion of cartilage in PBS was adopted in the current study to improve the signal quality. Although there was a possibility that the cartilage status might change during measurement due to evaporation of the water from the cartilage, two additional schemes were adopted to minimize this effect: the first scheme was that a sealed moistening environment was created in the container where PBS was filled below the cartilage-bone interface. It was assured that no PBS would cover the cartilage surface during the whole process of adjusting the surface inclination angles. The second scheme was that the tests at different inclination angles were completed first in each scan direction and then this process continued for the next scan direction. In one scan direction, the data collection was usually finished within two minutes. In such a short time, the change of the cartilage status was assumed to be minimal. Typically, all the tests in the four scan directions were completed within 10 minutes. However, with a further improved design of the OCT system including flexible gain adjustments, it is possible that the cartilage can be tested within bathing PBS, simulating a more physiological environment and the status of cartilage will then be better controlled during measurement.

4.3. Effects of surface inclinations

As expected, the surface inclination caused a dramatic change to the optical reflection from the surface (*ORC*). The slope of *ORC* with respect to the inclination angle in the intact cartilage (-2.02 dB/degree) was found to be similar to that in the glass slide, but was nearly double of that in the degraded cartilage (–0.94 dB/degree). Even a small angle of surface inclination (4º in the intact cartilage and 2º in the degraded cartilage from the experiments) would cause a significant reduction ($p < 0.05$) of *ORC*. This might be explained by that specular reflection is the main component contributing to the OCT signal from the surface of the intact cartilage while scattering might contribute much more to the OCT signal collected from the degraded tissue. The main change of *ORC* with the inclination angle came from the specular reflection because scattering is less angle dependent. In the intact cartilage, the decrease of amplitude may reach 20 dB at surface inclination of 10º. Therefore, it was found that *ORC* was the most sensitive parameter to the inclination angle. In contrast, *VSR* decreased only slightly as a function of the inclination angle. A smaller *VSR* shows that the surface becomes more homogenous concerning its optical properties. All the changes of *VSR* might be attributed to different *SNR* and proportions of the specular reflection and scattering among different inclination angles and between intact and degraded cartilages.

ORI value after mechanical degradation (18.5 ± 4.2 μm) was similar to ultrasonically determined corresponding index for surface roughness (*URI*) in a previous study (21.7 ± 3.2 μm) incorporating similar protocols in degrading the cartilage (Kaleva *et al.*, 2009). However, for the intact cartilage, *ORI* of this study (2.4 ± 0.7 μm) was much smaller than *URI* of that study (6.4 ± 1.3 μm), which was probably caused by a better resolution of the current OCT imaging compared to the ultrasound adopted in that study. *ORI* was found to increase as a function of the inclination angle in both intact and degraded groups. This might stem from the increased uncertainty in extracting the surface profile when quality of signal deteriorated with the increased inclination angle. Deteriorated quality of signal brought noise to the detection of the surface profile, causing an increase of *ORI*. As the reduction of signal quality with increased inclination angle was faster in the intact cartilage than that in the degraded cartilage, the slope of *ORI* versus angle was also larger in the intact cartilage.

As a parameter reflecting the properties of the internal cartilage tissue, *OBS* was found to be the most insensitive to the inclination angle. In this study, *OBS* was also compensated for the reflection at the cartilage/air interface. However, it should be noted that the energy compensation factor in the denominator of (7) was based on normal incidence of the optical beam, which was not true for those non-zero inclination angles. However, as energy reflection from this interface was very small (about 2%), the effect of this compensation on the final results was minimal and would not bias the findings of the current study. As expected, the angle dependence of *OBS* was the smallest among all the OCT parameters. This further confirmed that scattering dominated reflection in calculating *OBS* of the internal cartilage tissue. For convenience, a 500-point region was adopted in the study to compute the *OBS*. In practice, this dimension can be changed based on the size of the targeted region of interest, *e.g.* the superficial, the deep or the whole cartilage. The insensitivity of *OBS* on the inclination angle can be taken advantages over other parameters in a clinical diagnosis because it is difficult to assure a perpendicularity of the incident beam within a limited operation time in clinical situations.

4.4. Detection of cartilage degeneration

In this study, mechanical degradation of the cartilage surface was used to simulate the cartilage degeneration. It should be noted these artificial changes were not obvious with our direct view or conventional cameras, neither could these be used as a quantitative method to assess the severity of degeneration. All the parameters, except *OBS*, could detect the differences between the intact and mechanically degraded cartilages at an optimal inclination angle (0°). The degradation was induced on the cartilage surface through a mechanical grinding. Therefore, it was expected that no difference of the internal tissue status in terms of *OBS* was detected. This was also confirmed with histological images from the light microscopy. *ORC* was significantly ($p < 0.001$) larger in the intact cartilage than that in the degraded cartilage because the signal strength was dominated by specular reflection in the intact cartilage, while it was largely contributed by scattering in the degraded cartilage. However, if the measurement is not conducted in a perpendicular angle, conclusion may not be correct, for example, at the surface inclination of 10º. In this situation, the mean *ORC* is even larger in the degraded cartilage than that in the intact cartilage, although not reaching a significant level ($p = 0.12$). Therefore, it is necessary to control the incidence angle of the beam when using *ORC* for the characterization of degeneration of articular cartilage. In contrast to *ORC*, other two parameters *VSR* and *ORI* were quite robust to the inclination angle within the studied angles and could, in principle, differentiate the two groups for all the inclination angles. The change of roughness after grinding was confirmed with the SEM and light microscopy. Therefore, *ORI* can be used as a reliable estimate of the true roughness of the articular cartilage surface.

In practice, if one would like to mathematically correct the angle dependence of OCT parameters, proper counter-measures to detect minor degeneration of cartilage, such as small surface fibrillation, are required. The surface inclination, which could be used as the input for correction, can be estimated from OCT images. However, as the correction function also depends on the surface roughness, it is necessary to have an accurate estimation of the surface roughness, which makes the compensation quite complicated. Thus, proper mathematical corrections warrant further investigation.

In the future, articular cartilage optical model may be established using finite element analysis (FEA) in order to simulate how the measured optical parameters will change under varying surface roughness and material parameters. In this way, the strength and weakness of the quantitative characterization of articular cartilage using OCT could be conducted in a similar way as performed for ultrasound (Kaleva *et al.*, 2010). Optimally, the modeling results will be confirmed by experiments with spontaneously degenerated cartilage. Furthermore, all the OCT parameters could potentially be integrated with ultrasound parameters (Nieminen *et al.*, 2004), to define a combined index of cartilage quality to assess the degeneration status.

5. Conclusion

This study investigated the effects of surface non-perpendicularity and change in surface roughness on the four quantitative OCT parameters proposed for the characterization of articular cartilage. Results showed that *ORC* was the most sensitive while *OBS* was the most insensitive to the surface inclination. With a good control of perpendicularity or proper compensation mechanism, *ORC*, *VSR* and *ORI* have the potential to detect the degeneration of the cartilage surface, while *OBS* can be used to characterize the change of the internal cartilage tissue.

Acknowledgements

This work was supported in part by the Academy of Finland (Project 127198), Research Grant Council of Hong Kong (PolyU5354/08E) and the Hong Kong Polytechnic University (J-BB69).

The authors would also like to thank our colleagues Tuomas Viren, Antti Aula, Markus Malo and Dr. Hanna Isaksson in preparing the bovine samples and performing the experiment.

Conflict of interest

Authors have no conflicts of interest.

References

Adler R S, Dedrick D K, Laing T J, Chiang E H, Meyer C R, Bland P H and Rubin J M 1992 Quantitative assessment of cartilage surface roughness in osteoarthritis using high frequency ultrasound *Ultrasound Med. Biol.* **18** 51-8

Chiang E H, Adler R S, Meyer C R, Rubin J M, Dedrick D K and Laing T J 1994 Quantitative assessment of surface-roughness using backscattered ultrasound - the effect of finite surface curvature *Ultrasound Med. Biol.* **20** 123-35

Chu C R, Izzo N J, Irrgang J J, Ferretti M and Studer R K 2007 Clinical diagnosis of potentially treatable early articular cartilage degeneration using optical coherence tomography *J. Biomed. Opt.* **12** 051703

Chu C R, Lin D, Geisler J L, Chu C T, Fu F H and Pan Y T 2004 Arthroscopic microscopy of articular cartilage using optical coherence tomography *Am. J. Sports Med.* **32** 699-709

Chu C R, Williams A, Tolliver D, Kwoh C K, III S B and Irrgang J J 2010 Clinical optical coherence tomography of early articular cartilage degeneration in patients with degenerative meniscal tears *Arthritis Rheum.* **62** 1412-20

Davros W J, Zagzebski J A and Madsen E L 1986 Frequency-dependent angular scattering of ultrasound by tissue-mimicking materials and excised tissue *J. Acoust. Soc. Am.* **80** 229-37

Drexler W, Stamper D, Jesser C, Li X D, Pitris C, Saunders K, Martin S, Lodge M B, Fujimoto J G and Brezinski M E 2001 Correlation of collagen organization with polarization sensitive imaging of in vitro cartilage: implications for osteoarthritis *J. Rheumatol.* **28** 1311-8

Fanjul-Velez F and Arce-Diego J L 2010 Polarimetry of birefringent biological tissues with arbitrary fibril orientation and variable incidence angle *Opt. Lett.* **35** 1163-5

Forster H and Fisher J 1999 The influence of continuous sliding and subsequent surface wear on the friction of articular cartilage *Proc. Inst. Mech. Eng. Part H-J. Eng. Med.* **213** 329-45

Fournier C, Bridal S L, Berger G and Laugier P 2001 Reproducibility of skin characterization with backscattered spectra (12-25 MHz) in healthy subjects *Ultrasound Med. Biol.* **27** 603-10

Fujimoto J G, Pitris C, Boppart S A and Brezinski M E 2000 Optical coherence tomography: an emerging technology for biomedical imaging and optical biopsy *Neoplasia* **2** 9-25

Han C W, Chu C R, Adachi N, Usas A, Fu F H, Huard J and Pan Y 2003 Analysis of rabbit articular cartilage repair after chondrocyte implantation using optical coherence tomography *Osteoarthritis Cartilage* **11** 111-21

Herrmann J M, Pitris C, Bouma B E, Boppart S A, Jesser C A, Stamper D L, Fujimoto J G and Brezinski M E 1999 High resolution imaging of normal and osteoarthritic cartilage with optical coherence tomography *J. Rheumatol.* **26** 627-35

Hiro T, Leung C Y, Karimi H, Farvid A R and Tobis J M 1999 Angle dependence of intravascular ultrasound imaging and its feasibility in tissue characterization of human atherosclerotic tissue *Am. Heart J.* **137** 476-81

Jurvelin J, Kuusela T, Heikkila R, Pelttari A, Kiviranta I, Tammi M and Helminen H J 1983 Investigation of articular-cartilage surface-morphology with a semiquantitative scanning electron-microscopic method *Acta Anat.* **116** 302-11

Kaleva E, Liukkonen J, Toyras J, Saarakkala S, Kiviranta P and Jurvelin J S 2010 2-D finite difference time domain model of ultrasound reflection from normal and osteoarthritic human articular cartilage surface *IEEE Trans. Ultrason. Ferroelectr. Freq. Control* **57** 892-9

Kaleva E, Saarakkala S, Jurvelin J S, Viren T and Toyras J 2009 Effects of ultrasound beam angle and surface roughness on the quantitative ultrasound parameters of articular cartilage *Ultrasound Med. Biol.* **35** 1344-51

Li X D, Martin S, Pitris C, Ghanta R, Stamper D L, Harman M, Fujimoto J G and Brezinski M E 2005 High-resolution optical coherence tomographic imaging of osteoarthritic cartilage during open knee surgery *Arthritis Res. Ther.* **7** R318-23

Liu B, Harman M, Giattina S, Stamper D L, Demakis C, Chilek M, Raby S and Brezinski M E 2006 Characterizing of tissue microstructure with single-detector polarization-sensitive optical coherence tomography *Appl. Opt.* **45** 4464-79

Nieminen H J, Saarakkala S, Laasanen M S, Hirvonen J, Jurvelin J S and Toyras J 2004 Ultrasound attenuation in normal and spontaneously degenerated articular cartilage *Ultrasound Med. Biol.* **30** 493-500

Pan Y T, Li Z G, Xie T Q and Chu C R 2003 Hand-held arthroscopic optical coherence tomography for *in vivo* high-resolution imaging of articular cartilage *J. Biomed. Opt.* **8** 648-54

Patel N A, Zoeller J, Stamper D L, Fujimoto J G and Brezinski M E 2005 Monitoring osteoarthritis in the rat model using optical coherence tomography *IEEE Trans. Med. Imaging* **24** 155-9

Picano E, Landini L, Distante A, Salvadori M, Lattanzi F, Masini M and Labbate A 1985 Angle dependence of ultrasonic backscatter in arterial tissues - a study *in vitro Circulation* **72** 572-6

Rogowska J and Brezinski M E 2002 Image processing techniques for noise removal, enhancement and segmentation of cartilage OCT images *Phys. Med. Biol.* **47** 641-55

Rogowska J, Bryant C M and Brezinski M E 2003 Cartilage thickness measurements from optical coherence tomography *J. Opt. Soc. Am. A - Opt. Image Sci. Vis.* **20** 357-67

Saarakkala S, Toyras J, Hirvonen J, Laasanen M S, Lappalainen R and Jurvelin J S 2004 Ultrasonic quantitation of superficial degradation of articular cartilage *Ultrasound Med. Biol.* **30** 783-92

Saarakkala S, Wang S Z, Huang Y P and Zheng Y P 2009 Quantification of optical surface reflection and surface roughness of articular cartilage using optical coherence tomography *Phys. Med. Biol.* **54** 6837-52

Ugryumova N, Jacobs J, Bonesi M and Matcher S J 2009 Novel optical imaging technique to determine the 3-D orientation of collagen fibers in cartilage: variable-incidence angle polarization-sensitive optical coherence tomography *Osteoarthritis Cartilage* **17** 33-42

Waag R C, Lee P P K, Persson H W, Schenk E A and Gramiak R 1982 Frequency-dependent angle scattering of ultrasound by liver *J. Acoust. Soc. Am.* **72** 343-52

Wang S Z, Huang Y P, Saarakkala S and Zheng Y P 2010a Quantitative assessment of articular cartilage with morphologic, acoustic and mechanical properties obtained using high frequency ultrasound *Ultrasound Med. Biol.* **36** 512-27

Wang S Z, Huang Y P, Wang Q, Zheng Y P and He Y H 2010b Assessment of depth and degeneration dependences of articular cartilage refractive index using optical coherence tomography *in vitro Connect. Tissue Res.* **51** 36-47

Xie T Q, Guo S G, Zhang J, Chen Z P and Peavy G M 2006a Determination of characteristics of degenerative joint disease using optical coherence tomography and polarization sensitive optical coherence tomography *Lasers Surg. Med.* **38** 852-65

Xie T Q, Guo S G, Zhang J, Chen Z P and Peavy G M 2006b Use of polarization-sensitive optical coherence tomography to determine the directional polarization sensitivity of articular cartilage and meniscus *J. Biomed. Opt.* **11** 064001

Xie T Q, Xia Y, Guo S G, Hoover P, Chen Z P and Peavy G M 2008 Topographical variations in the polarization sensitivity of articular cartilage as determined by polarization-sensitive optical coherence tomography and polarized light microscopy *J. Biomed. Opt.* **13** 054034

Figure captions

Figure 1. The setup for osteochondral disk measurement. A1 & A2: two manual linear translation stages which adjust the horizontal position of the testing point; B: a manual goniometer which controls the surface inclination angle; C: a manual rotary stage which changes the scan direction. The four scan directions in one disk are also shown on the upper right corner.

Figure 2. (a), (b) & (c) represent typical OCT images from intact cartilage at 0º inclination, intact cartilage at 10º inclination and mechanically degraded cartilage at 0º inclination, respectively. Width of the images is 1 mm. Various OCT parameters calculated from the images are denoted on top of the images. A definition of 'noise window' and 'cartilage window' is shown in (a). The noise level estimated from the noise window and the signal level from the cartilage window are used to define the abrupt jump of the signal due to the cartilage surface. The line covering the cartilage surface indicates the original surface profile detected. The two lines below the surface indicate the 500-point ROI for calculation of *OBS*. (d) & (e) are typical surface profiles before and after filtering which are extracted from the typical OCT images shown in (a), (b) & (c). The filtering is based on smoothed surface profiles as shown in (d) by lines without markers. The effects of surface curvature and inclination have been removed in (e) in comparison with (d) for extraction of the true surface roughness.

Figure 3. The relationship between *ORC* and the angle of surface inclination. Error bars indicate standard deviations. For a clearer view, the curve for the degraded cartilage after mechanical grinding is shifted by a step of 0.2 in the *x*-axis. *ORC* decreases with the increase of the surface inclination angle. At angle 0°, *ORC* is significantly larger in the intact cartilage than that after surface degradation.

Figure 4. The relationship between *VSR* and the angle of surface inclination. Error bars indicate standard deviations. *VSR* generally decreases with the increase of the surface inclination angle, but this is not so obvious in the degraded cartilage. At angle 0°, *VSR* is significantly smaller in the intact cartilage than that after surface degradation.

Figure 5. The relationship between *ORI* and the angle of surface inclination. Error bars indicate standard deviations. *ORI* increases with the increase of the surface inclination angle. At angle 0°, *ORI* is significantly smaller in the intact cartilage than that in the degraded state.

Figure 6. The relationship between *OBS* and the angle of surface inclination. Error bars indicate standard deviations. For a clearer view, the curve for the degraded cartilage after mechanical grinding is shifted by a step of 0.2 in the *x*-axis. *OBS* generally decreases with the increase of the surface inclination angle. The change of *OBS* before and after mechanical degradation of the surface is nonsignificant.

Figure 7. Typical SEM images from (a) an intact cartilage surface and (b) a mechanically degraded cartilage surface. A large increase of the surface roughness induced by the mechanical grinding is clearly observed here.

Figure 8. Typical light microscopy images for the Safranin O red staining of (a) an intact cartilage slice and (b) a mechanically degraded cartilage slice with the subchondral bone. There is no obvious change of PG content after the mechanical grinding. However, surface irregularities are clearly observed after grinding.

Figures

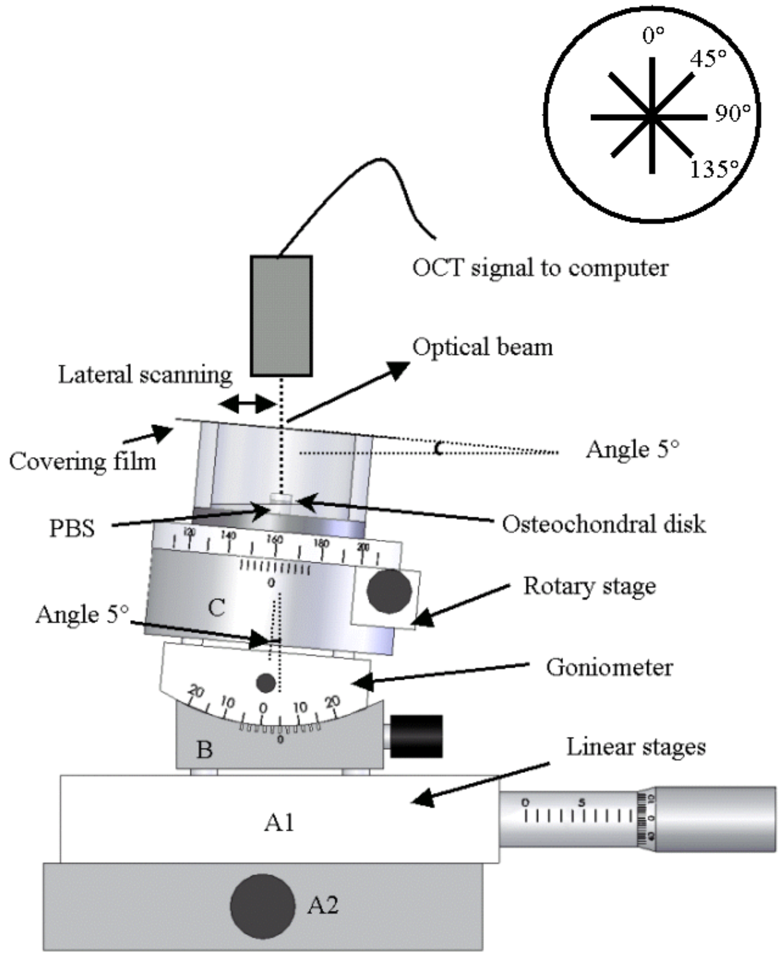

Figure 1.

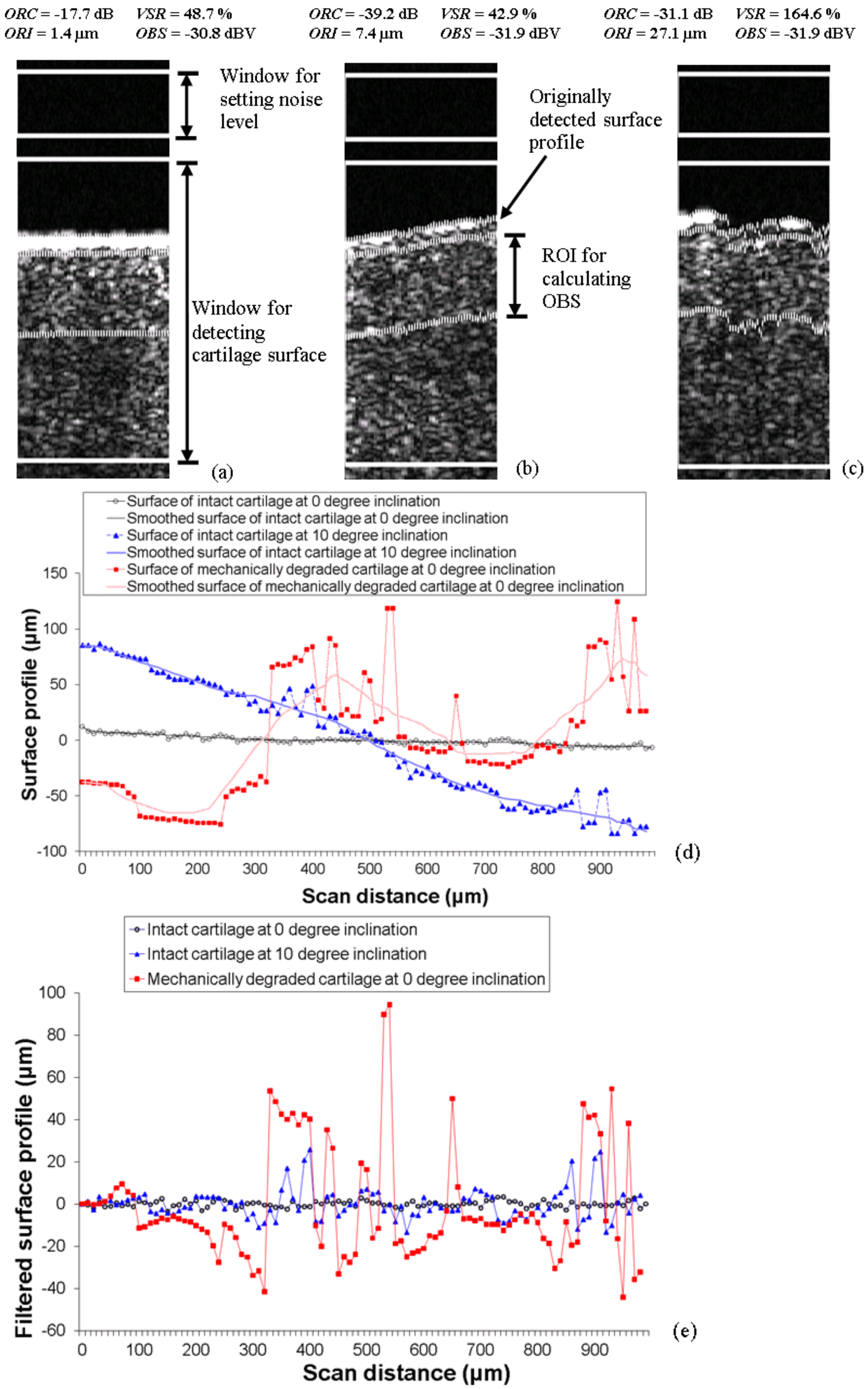
ORC = -17.7 dB
VSR = 48.7 %
ORI = 1.4 μm
OBS = -30.8 dBV
ORC = -39.2 dB
VSR = 42.9 %
ORI = 7.4 μm
OBS = -31.9 dBV
ORC = -31.1 dB
VSR = 164.6 %
ORI = 27.1 μm
OBS = -31.9 dBV
Window for setting noise level
Window for detecting cartilage surface
Originally detected surface profile
ROI for calculating OBS
(a)
(b)
(c)
Surface of intact cartilage at 0 degree inclination
Smoothed surface of intact cartilage at 0 degree inclination
Surface of intact cartilage at 10 degree inclination
Smoothed surface of intact cartilage at 10 degree inclination
Surface of mechanically degraded cartilage at 0 degree inclination
Smoothed surface of mechanically degraded cartilage at 0 degree inclination
Surface profile (μm)
Scan distance (μm)
(d)
Intact cartilage at 0 degree inclination
Intact cartilage at 10 degree inclination
Mechanically degraded cartilage at 0 degree inclination
Filtered surface profile (μm)
Scan distance (μm)
(e)

Figure 2.

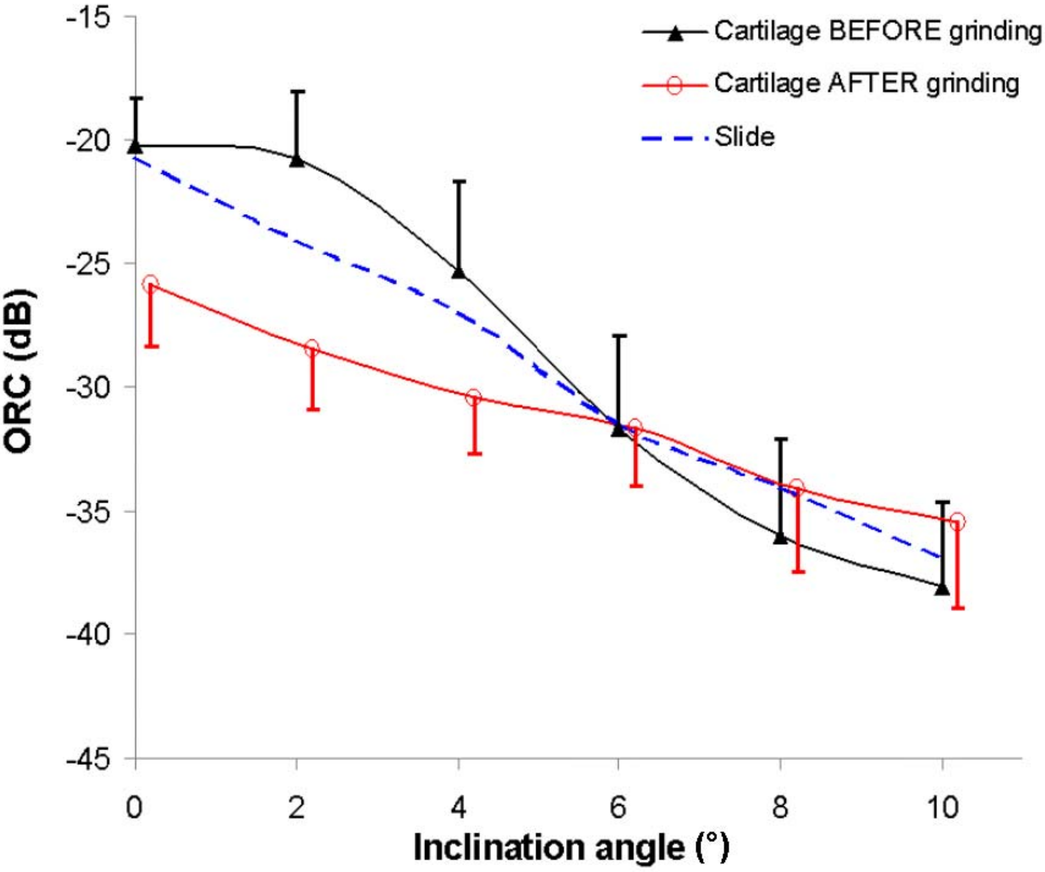

Cartilage BEFORE grinding
Cartilage AFTER grinding
Slide
ORC (dB)
-15
-20
-25
-30
-35
-40
-45
0
2
4
6
8
10
Inclination angle (°)

Figure 3.

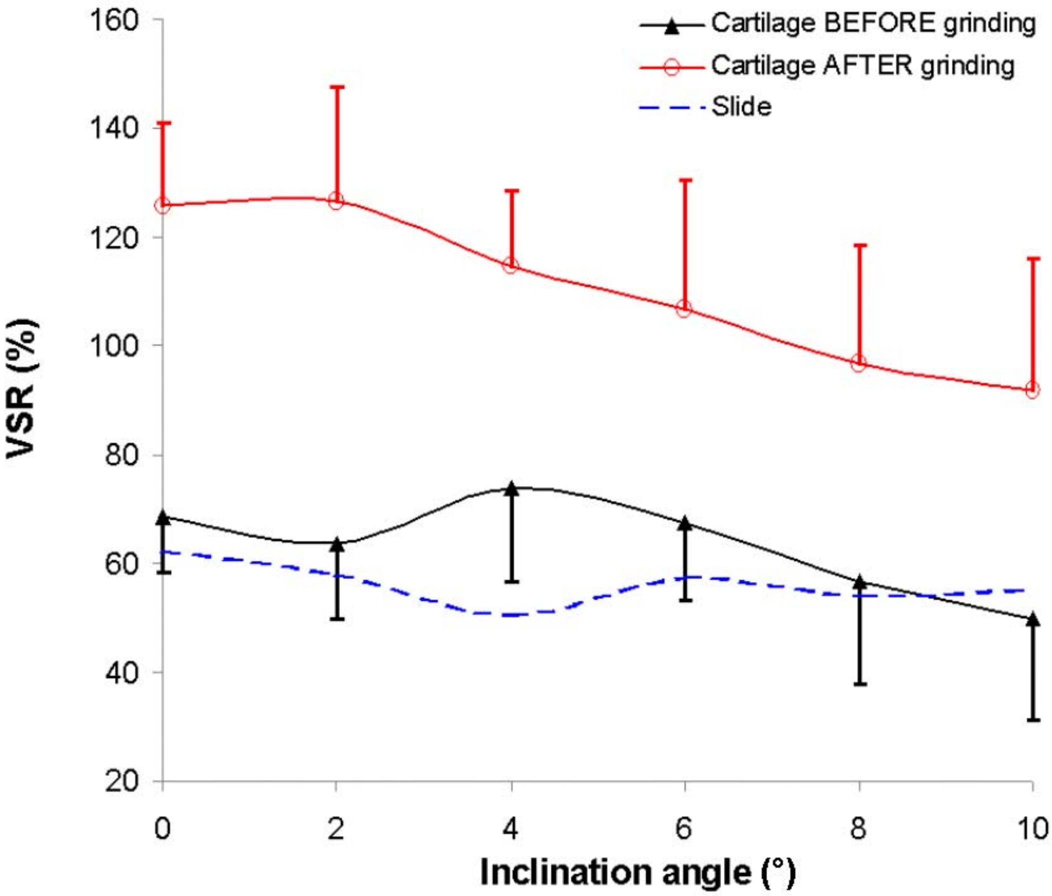
Cartilage BEFORE grinding
Cartilage AFTER grinding
Slide
VSR (%)
160
140
120
100
80
60
40
20
0
2
4
6
8
10
Inclination angle (°)

Figure 4.

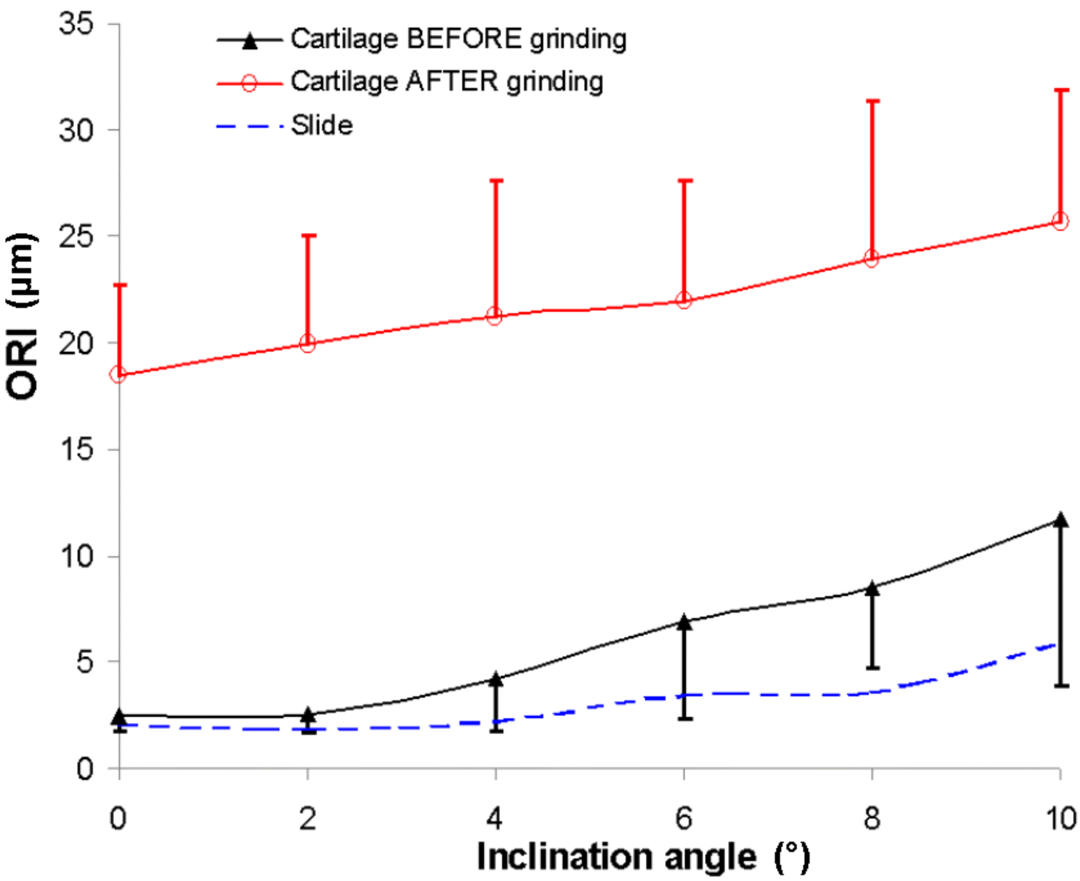
Cartilage BEFORE grinding
Cartilage AFTER grinding
Slide
ORI (µm)
35
30
25
20
15
10
5
0
0
2
4
6
8
10
Inclination angle (°)

Figure 5.

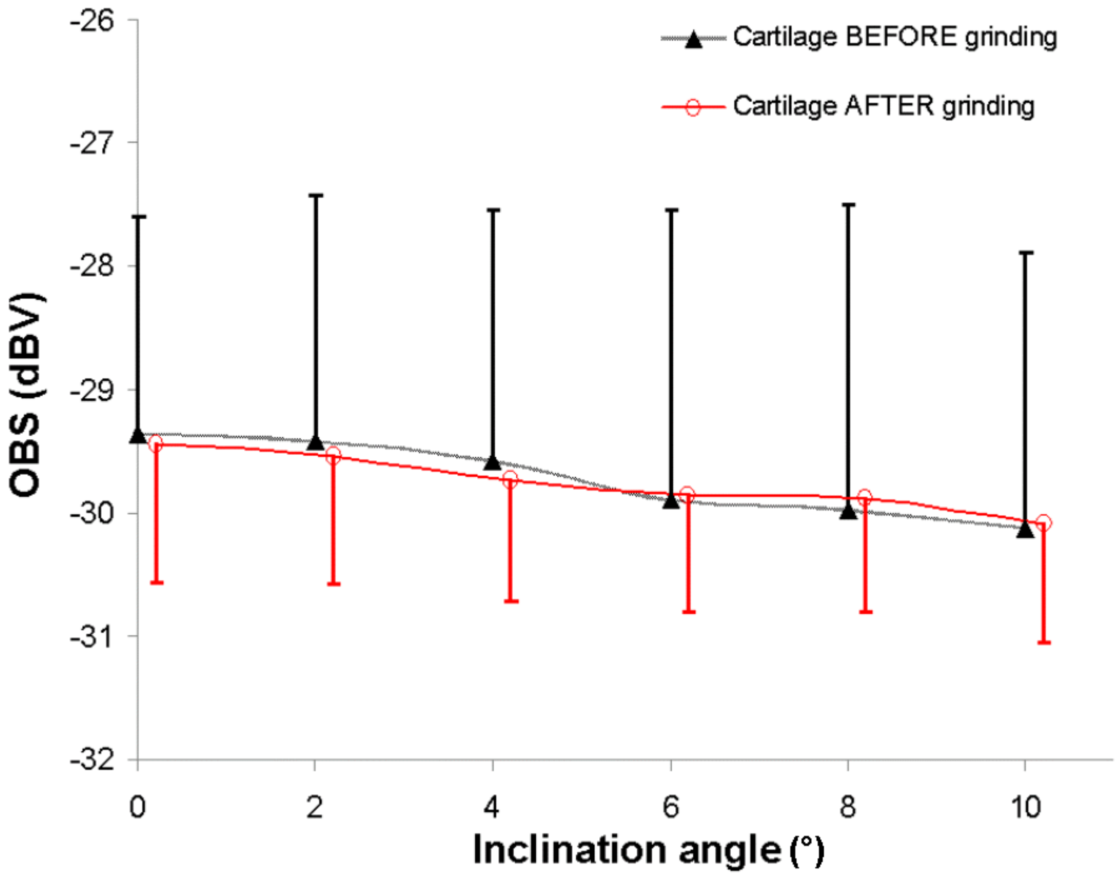
Cartilage BEFORE grinding
Cartilage AFTER grinding
OBS (dBV)
-26
-27
-28
-29
-30
-31
-32
0
2
4
6
8
10
Inclination angle (°)

Figure 6.

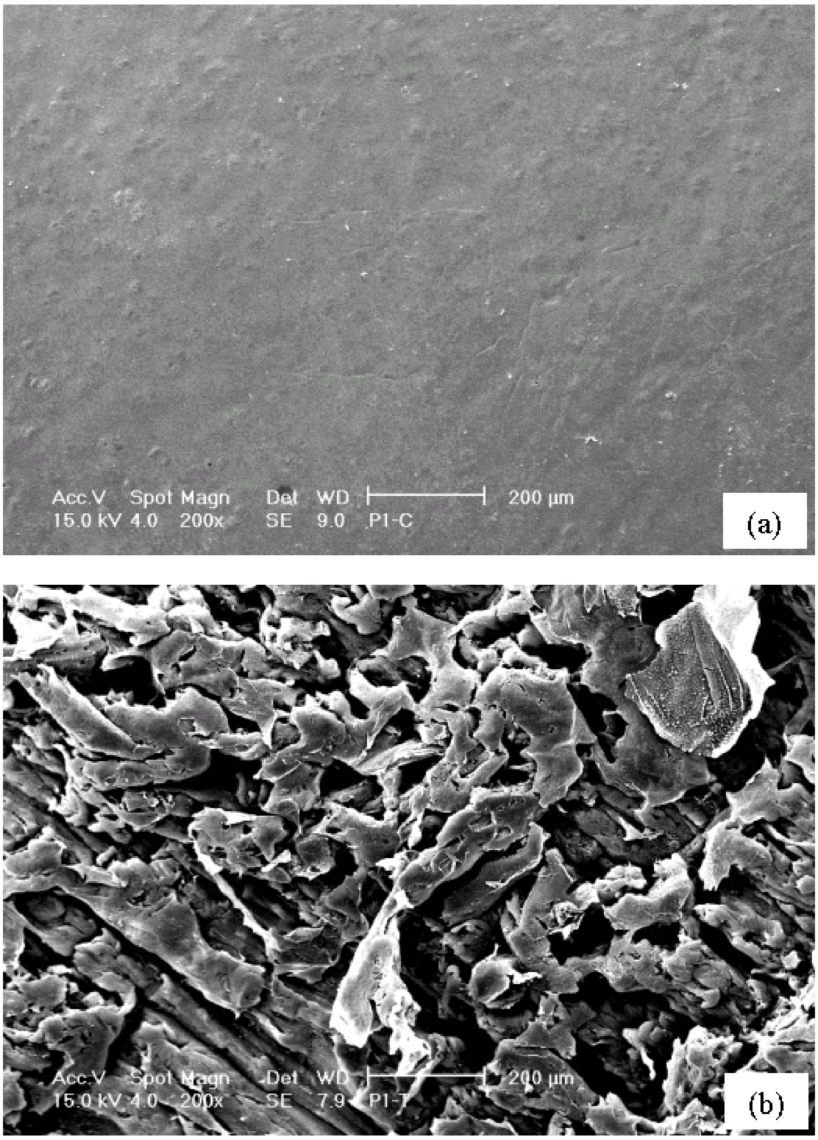
Acc.V Spot Magn Det WD 200 µm
15.0 kV 4.0 200x SE 9.0 PI-C
(a)
Acc.V Spot Magn Det WD 200 µm
15.0 kV 4.0 200x SE 7.9 PI-T
(b)

Figure 7.

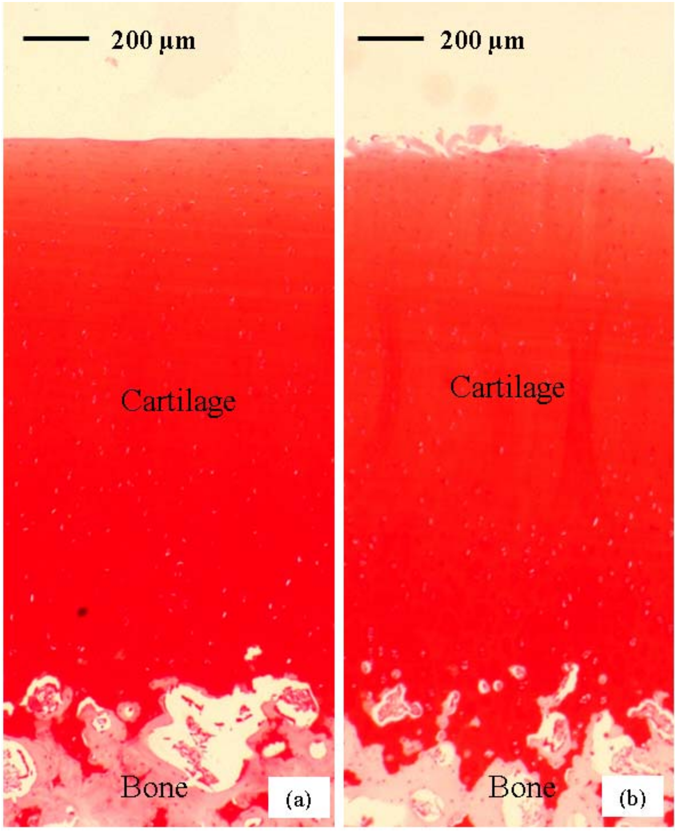

Figure 8.

Table 1 Statistical analysis (paired-sample *t*-test) of comparisons at two angles.

OCT parameters		2° vs 0°	4° vs 0°	6° vs 0°	8° vs 0°	10° vs 0°
ORC	Intact	<	< (**)	< (***)	< (***)	< (***)
	Degraded	< (***)	< (***)	< (**)	< (***)	< (***)
VSR	Intact	<	>	<	< (**)	< (**)
	Degraded	>	<	<	<	< (*)
ORI	Intact	>	> (*)	> (*)	> (***)	> (**)
	Degraded	>	>	> (*)	> (*)	> (**)
OBS	Intact	<	<	<	<	< (*)
	Degraded	<	< (*)	<	< (*)	< (*)

Significant levels of statistical analyses: * $p < 0.05$; ** $p < 0.01$; *** $p < 0.001$

Table 2 Comparisons of various OCT parameters at inclination angle of 0º between intact and degraded cartilages. *ORC* becomes significantly smaller, while *VSR* and *ORI* become significantly larger after mechanical degradation. However, no significant change of *OBS* is observed after mechanical degradation. Histology also showed a significantly larger roughness after mechanical degradation.

Materials	*ORC* (dB)	*VSR* (%)	Surface roughness (μm)		*OBS* (dBV)
			ORI	Histology	
Intact	-20.2 (1.9)	68.7 (10.2)	2.4 (0.7)	2.0 (0.5)	-29.4 (1.8)
Degraded	-25.9*** (2.5)	125.8*** (15.2)	18.5*** (4.2)	20.1*** (6.3)	-29.4 (1.1)
Slide	-20.7	62.1	2.0	N.A.	N.A.

Value in parentheses indicate standard deviation. *** $p < 0.001$ compared to intact cartilage. N.A.: not available